AGU PUBLICATIONS

Geophysical Research Letters

RESEARCH LETTER
10.1002/2017GL074895

Key Points:
- Magnetospheric response to small shocks not typical bipolar electric field pulse seen for large shocks
- Propagation of compression on VAP, MMS, and GOES-13 is consistent with fast mode speed; large-scale structure is not fast mode
- Electric field pulse associated with small shock energizes electrons to >50 keV; flux enhancements seen up to several MeV

Correspondence to:
C. Cattell,
cattell@umn.edu

Citation:
Cattell, C., et al. (2017), Dayside response of the magnetosphere to a small shock compression: Van Allen Probes, Magnetospheric MultiScale, and GOES-13, *Geophys. Res. Lett.*, *44*, 8712–8720, doi:10.1002/2017GL074895.

Received 10 JUL 2017
Accepted 8 AUG 2017
Accepted article online 10 AUG 2017
Published online 9 SEP 2017

Dayside response of the magnetosphere to a small shock compression: Van Allen Probes, Magnetospheric MultiScale, and GOES-13

C. Cattell[1], A. Breneman[1], C. Colpitts[1], J. Dombeck[1], S. Thaller[1], S. Tian[1], J. Wygant[1], J. Fennell[2], M. K. Hudson[3], Robert Ergun[4], C. T. Russell[5], Roy Torbert[6], Per-Arne Lindqvist[7], and J. Burch[8]

[1]School of Physics and Astronomy, University of Minnesota, Twin Cities, Minneapolis, Minnesota, USA, [2]Aerospace Corporation, El Segundo, California, USA, [3]Department of Physics and Astronomy, Dartmouth College, Hanover, New Hampshire, USA, [4]LASP, University of Colorado Boulder, Boulder, Colorado, USA, [5]IGPP, UCLA, California, Los Angeles, USA, [6]EOS, University of New Hampshire, Durham, New Hampshire, USA, [7]KTH, Stockholm, Sweden, [8]SWRI, San Antonio, Texas, USA

Abstract Observations from Magnetospheric MultiScale (~8 *Re*) and Van Allen Probes (~5 and 4 *Re*) show that the initial dayside response to a small interplanetary shock is a double-peaked dawnward electric field, which is distinctly different from the usual bipolar (dawnward and then duskward) signature reported for large shocks. The associated $E \times B$ flow is radially inward. The shock compressed the magnetopause to inside 8 *Re*, as observed by Magnetospheric MultiScale (MMS), with a speed that is comparable to the $E \times B$ flow. The magnetopause speed and the $E \times B$ speeds were significantly less than the propagation speed of the pulse from MMS to the Van Allen Probes and GOES-13, which is consistent with the MHD fast mode. There were increased fluxes of energetic electrons up to several MeV. Signatures of drift echoes and response to ULF waves also were seen. These observations demonstrate that even very weak shocks can have significant impact on the radiation belts.

Plain Language Summary Very fast moving clouds of charged particles are ejected from the Sun when it is active. Shock waves often develop at the cloud front as it plows through the solar wind. When the shock hits the Earth's magnetic field, it can push the Earth's magnetic shield inside the distance where many communication and weather satellites orbit. The energy associated with the shock can also very rapidly increase the energy of electrons trapped in the Earth's magnetic field in the Van Allen Radiation belts. These electrons can damage satellites. We have used four satellites arrayed at different locations on the dayside of the Earth's magnetic field to show, for the first time, that small shocks have a different effect than the large shocks that are usually studied but that even small shocks can produce relativistic electrons.

1. Introduction

The very strong shock observed by CRRES on 24 March 1991 [*Wygant et al.*, 1994] that resulted in the formation of a new radiation belt has provided the prototypical example of the magnetospheric response to an interplanetary (IP) shock compression. The electric field, observed on the nightside, had a large (~40 mV/m) bipolar pulse of ~2 min duration, first dawnward and then duskward, consistent with antisunward flow as the magnetosphere was compressed and sunward flow in association with the relaxation. The inferred field near noon was approximately 200 mV/m. Similar bipolar pulses with amplitudes of ~10 mV/m and durations of several minutes have been reported in association with other shock compressions [*Kim et al.*, 2012; *Foster et al.*, 2015] and in MHD simulations [*Kress et al.*, 2007; *Hudson et al.*, 2015; *Paral et al.*, 2015]. The bipolar electric field has been interpreted to be associated with the excitation of a fast mode wave that propagates primarily azimuthally. Electrons in drift resonance with the fast mode wave electric field are promptly accelerated [*Wygant et al.*, 1994; *Li et al.*, 1993], which can result in drift echoes and sometimes the creation of a new radiation belt.

For a moderate shock on 8 October 2013, *Foster et al.* [2015] estimated the propagation speed to be about 850 km/s from the observed delay times between the Van Allen Probes spacecraft, which was comparable to the event simulation [*Hudson et al.*, 2015; *Paral et al.*, 2015]. *Schmidt and Pedersen* [1988], in a statistical study of sudden commencements using GEOS data, found radial propagation speeds of ~950 km/s and azimuthal speeds of ~1100 km/s. *Samsonov et al.* [2014], in a study of velocity perturbations in the dayside

magnetosphere during eight sudden impulse (SI) events, concluded that the observed initial oscillations were Alfvenic with electric fields of a few to ~9 mV/m, and both the waves and magnetic compressions were consistent with simulations.

In this letter, we present observations of the initial dayside response of the magnetosphere to a small interplanetary shock. Satellites on the dayside measured a double-peaked dawnward electric field, distinctly different from the usual bipolar field seen for large shocks and in simulations but with a comparable duration. Energization of electrons is observed but to lower energies and fluxes than for large shocks. This study demonstrates that it is necessary to understand the magnetospheric response to shocks of all sizes to characterize radiation belt dynamics. The data sets and event overview are presented timing of propagation, comparison to fast mode and Alfven speeds, and response of energetic particles are described in section 2. Discussion and conclusions are in section 4.

2. Data Sets and Event Summary

On 14 December 2015, a small IP shock transited ACE at 12:31 UT, Wind at 12:41 UT, and lunar orbit at 13:10 UT, as observed by ARTEMIS (THEMIS-B and THEMIS-C), respectively, 47 *Re* and 48 *Re* upstream of the model magnetopause location, at a local time of 14:30 LT. Using the OMNI delayed data, the estimated shock impact on the magnetopause was 13:18. The initial increase in the dynamic pressure was a factor of 3, from 2 to 6 nPa (see Figure 1b, fifth panel), and was associated with primarily southward interplanetary magnetic field. There was a brief decrease in the pressure after the initial pulse, followed at 14:30 UT by a larger pressure increase through 19:00 UT (not shown; occurred after the interval discussed in this report). Herein, we focus on the initial compression at 13:18 UT. The shock normal had a significant *y* component at ACE, Wind, and ARTEMIS, suggesting that the shock may have impacted the magnetosphere at an angle.

Figure 1a plots the locations at 13:20 of the Van Allen Probes, Magnetospheric MultiScale (MMS) and GOES-13, which were well arrayed to characterize the dayside response to the shock-associated compression. The MMS satellites were closest to the magnetopause. Van Allen Probe A (VAP-A) and GOES-13 were farther from the magnetopause. Van Allen Probe B (VAP-B), which was closest to the Earth, entered the plasmasphere at 12:30 UT, where it remained throughout the event. Note that MMS and VAP observed strong electromagnetic ion cyclotron (EMIC) waves in association with the relaxation of the magnetosphere [*Capman et al*., 2016], as has been reported for compressions [*Anderson and Hamilton*, 1993].

The primary data sets utilized in this study are the quasi-static electric and magnetic field measurements from the two Van Allen Probes [*Wygant et al*., 2013; *Kletzing et al*., 2013] and from the four MMS satellites [*Burch et al*., 2015; *Russell et al*., 2014; *Torbert et al*., 2015; *Lindqvist et al*., 2015]. In addition, we examine particle data from the REPT [*Baker et al*., 2012], MagEIS (Magnetic Electron and Ion Spectrometer) [*Blake et al*., 2013], and HOPE [*Funsten et al*., 2013] particle detectors on the Van Allen Probes [*Spence et al*., 2013], and the particle and magnetic field data from GOES-13 [*Singer et al*., 1996]. Data on the solar wind conditions and interplanetary shock were obtained from ACE [*Stone et al*., 1998], Wind [*Lepping et al*., 1995], and THEMIS-B and -C [*Angelopoulos*, 2008; *McFadden et al*., 2008].

The initial magnetospheric response on the dayside was observed at ~13:20 by Magnetospheric Multiscale (MMS) and Van Allen Probe A, ~13:20:20 at Van Allen Probe B, and at ~13:23 at GOES-13 as can be seen in Figure 1b, which plots the magnitude of the magnetic field from MMS1 (green), VAP-A (blue), and GOES-13 (purple) in the first panel, the next three panels plot the duskward (E_y) component of the electric field from MMS1, VAP-A, and VAP-B, and the OMNI solar wind dynamic pressure and *SYM-H* (divided by 10) in the bottom panel. In response to the shock impact, MMS, VAP-A, and VAP-B all observed a dawnward electric field pulse with a double peaked structure (note the different scale for MMS1), in association with the compression in the total magnetic field. The sudden drop in the magnetic field observed by MMS was due to the fact that MMS crossed the magnetopause into the sheath at ~13:23:30 and back into the magnetosphere at ~13:25:15. Thus, the magnetopause boundary was inside 8 *Re* (*X*gsm of ~7.7 *Re*) at a LT of ~13. The compression in the magnetic field and the decrease in E_y at MMS begins at ~13:20:15, followed by the magnetic field compression and E_y signal at VAP-A and VAP-B. The double-peaked E_y signal is seen on MMS, while it is still inside the magnetosphere.

The timing of the pulse, and thus the propagation speed, is most accurately determined from the magnetic field signatures, because the time resolution of the electric field measurement on VAP-A was reduced due to

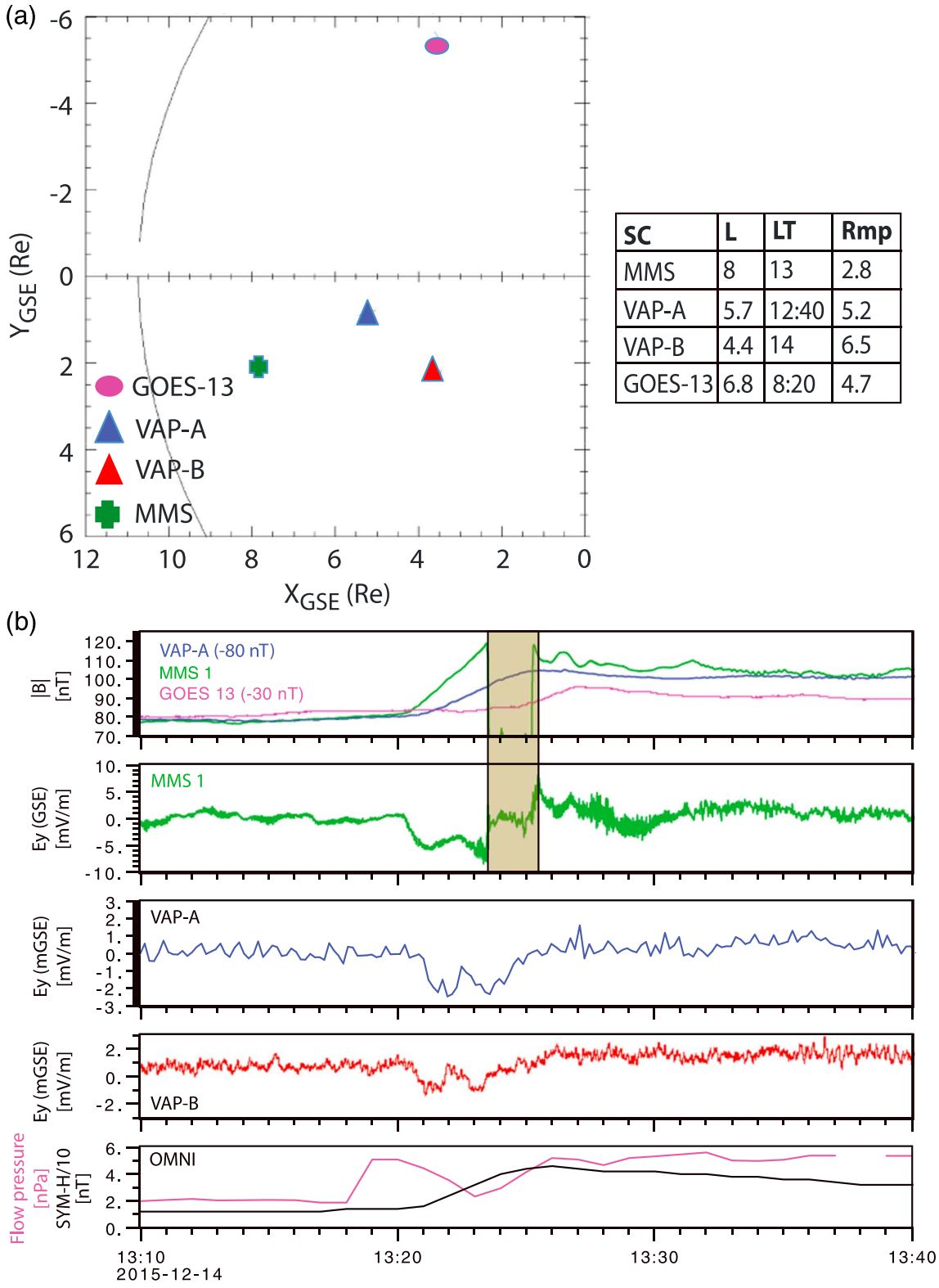

SC	L	LT	Rmp
MMS	8	13	2.8
VAP-A	5.7	12:40	5.2
VAP-B	4.4	14	6.5
GOES-13	6.8	8:20	4.7

Figure 1. (a) Satellite locations at ~13:20 on 14 December 2015. (b, first panel) Btotal on VAP-A (−80 nT) in blue, on MMS1 in green, and on GOES-13 (−35 nT) in purple. Note that the rapid change seen on MMS at ~13:25 is a crossing into the magnetosheath and back into the magnetosphere. (b, second panel) E_y on MMS1. (b, third panel) E_y on VAP-A (spin period resolution due to loss of one spherical probe). (b, fourth panel) E_y on on VAP-B. (b, fifth panel) solar wind pressure (purple) and *SYM-H* (divided by 10, black).

Table 1. Compression Speed Determination

Method	Delay, s	Speed, km/s	Normal
SC pairs B_z			*along sep. vector in *x-y*
MMS-VAP-A	12–18	1020–1530	In and dusk
MMS-VAP-B	12–20	1340–2240	In
VAP-A-VAP-B	4–11	1200–3200	In and dawn
4 SC		1250–1500	(−0.9, −0.3, and +0.1)

the loss of measurements from one probe. Note that GOES-13 initially observed a slight decrease in the magnetic field (~2 min after the compression at MMS), followed by the compression (~4 min after MMS). Table 1 shows the range of delay times in B_z between spacecraft pairs, and the resulting propagation speeds along the separation vector. The impulse propagation speed and direction can also be estimated (assuming a plane wave), using magnetic field data (B_z and B_{tot}) from the four dayside satellites (MMS-1, VAP-A, VAP-B, and GOES-13), shown in the bottom row of Table 1. Speeds are in the range of 1200 to 1500 km/s, and generally radially inward and toward dawn. As discussed below, this in consistent with the fast mode speed.

The most accurate density estimates are obtained from the upper hybrid line, which is used to calibrate the density obtained from the spacecraft potential [*Kurth et al.*, 2015]. During the magnetic field compression, the density ranges from ~10 cm^{-3} to 30 cm^{-3} on VAP-A and ~100 cm^{-3} to 120 cm^{-3} on VAP-B. On both satellites, the ion density (for energies >30 eV) is <~1, indicating that most of the density is cold plasma. There is significant oxygen (O+/H+ of ~0.2 to 0.4 on VAP-A and ~0.5 to 1 on VAP-B). Using these values, the range of the Alfven speed is ~700 km/s to 1200 km/s for VAP-A and 600 km/s to 900 km/s for VAP-B. The Alfven speed at MMS is ~800 to 1200 km/s for n ~ 5 cm^{-3} (based on the upper hybrid line). Using the observed electron temperatures from HOPE, we can calculate the sound speed (C_{sA} = 540 km/s and C_{sB} = 370 km/s), and thus the fast mode speed, ~806 km/s to 1350 km/s on VAP-A and 620 km/s to 950 km/s on VAP-B. Thus, the observed propagation speeds are consistent with fast mode. It should be noted, however, that there is not a significant difference between the range of fast mode speeds and the range of Alfven speeds for this event.

The delay time from the estimated time of impact of the shock on the magnetopause to the initial compression on each satellite is also of interest. Given the 1 min resolution of the OMNI data, the delay between the shock arrival at the magnetopause and at MMS ranges from ~1 to 2 min. The speeds for a range of model magnetopause locations, based on solar wind pressures from 0 to 6 nPa, range from ~50 km/s to a few 100 km/s. These speeds are much lower than the Alfven speed and the sound speed. Although the estimated shock impact time is not well determined, it should be accurate to within ~1 min; even with a shorter delay, the speeds are subsonic.

The usual interpretation of the observed response to a shock compression is a fast mode wave; therefore, one would expect to see an increase in density associated with the enhanced magnetic field. Figure 2 (top) shows that this is not the case. Figure 2 (bottom) shows that density is essentially all due to cold plasma. It is clear that for most of the large-scale compression, from ~13:23 to ~13:30 when the change in the magnetic field magnitude is ~20–30 nT, there was a density decrease to ~10 cm^{-3}. This suggests that the large-scale structure is slow mode or in pressure balance, although the small-scale waves may be fast mode. Note that there was an increase in the electron density observed by HOPE. Because VAP-B was inside the plasmasphere during the interval of interest, it is difficult to assess the significance of the relationship of the density changes to the magnetic field changes.

At both Van Allen Probes, there were increases in the energetic electron fluxes, in association with the electric field signal and compression, as shown in Figure 3a, which plots selected channels of the electrons at 90° pitch angle from MagEIS for both spacecraft. The top panel shows the ~30 keV and ~54 keV channels; the bottom panel shows the ~75 keV and ~100 keV. An interesting feature seen on VAP-A is that the enhanced flux is larger for the 54 keV channel than for the 31 keV channel. This feature is not seen on VAP-B. The 80 keV channel on VAP-A is also strongly enhanced. MMS (not shown) observed slight increase only in the 40 keV channel. If the energization from inward electron transport due to the shock-induced electric field pulse is interpreted to be adiabatic [*Wygant et al.*, 1994], the source population would have been at L = 5.85–6 and resulted in an energy increase by 1.3–1.6 times, corresponding to an energy of ~35 to 40 keV for the largest enhancement at 54 keV. The drift speed of particles at these energies is much too low to be resonant with the azimuthal propagation of the pulse [*Li et al.*, 1993; *Wygant et al.*, 1994].

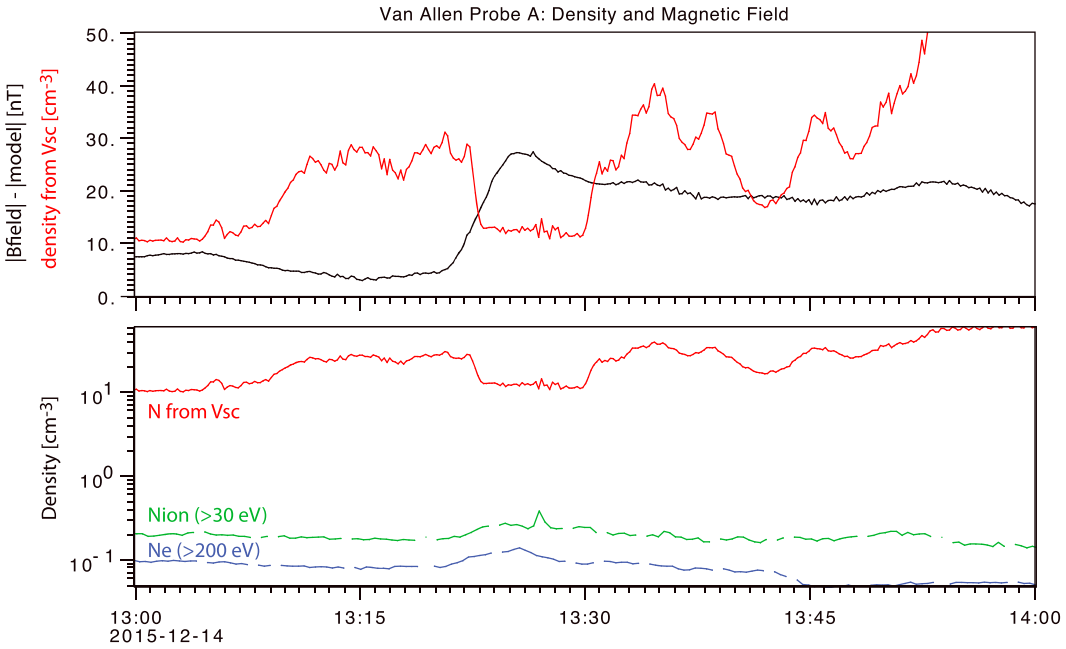

Figure 2. Comparison of magnetic field magnitude and density at VAP-A. (top) The magnitude of the magnetic field—model field in black and the density from the spacecraft potential in red. (bottom) The density from the spacecraft potential in red, the density of ions >30 eV from HOPE in green, and the density of electrons >200 eV from HOPE in blue.

Comparison of VAP-A and GOES-13 electrons is presented in Figure 3b. Both satellites observed slight (~60%) increases in fluxes at high energies (~1 MeV). GOES-13 observed increases in fluxes over the energy range from ~40 keV to 150 keV, with a weak decrease in fluxes at higher energies (275 and 475 keV). Both Van Allen Probes observed increases in fluxes at energies up to ~5 MeV. On GOES-13 there were enhancements to >2 MeV. Drift echoes occurred on Van Allen Probe A, most clearly in energies from about 200 to 500 keV. Above this energy, there may be drift echoes but they are masked by the larger response to the ULF waves that occur after the shock impact.

The magnetic field from the four MMS satellites can be analyzed to determine the magnetopause boundary normal and speed at the crossings out of and then into the magnetosphere. For the initial crossing, the normal was primarily along X_{gse} with a small negative Y_{gse} component and the speed was ~40 km/s. This speed is quite comparable to the $E \times B/B^2$ velocity at MMS during the compression, ~40 to 60 km/s; it is much slower than the fast mode speed throughout the dayside magnetosphere, suggesting that the motion of the magnetopause was governed by the plasma flow and pressure balance rather than a fast mode wave. During the subsequent expansion, the normal was almost totally in the *X* direction, and the speed was ~25 km/s. The duration of the magnetic field compression at MMS is ~3.5 min. At 50 km/s, this would correspond to ~1.6 *Re*, which is very similar to the distance to the model magnetopause obtained for an enhanced solar wind pressure of 4 nPa. Thus, the observations are consistent with a picture of the compression of the magnetopause by a slow piston with the magnetopause location essentially set by pressure balance. The initial magnetopause current sheet crossing at MMS lasted ~35 s, corresponding to a scale size of ~0.2 to 0.3 *Re*.

On all three satellites, the *y* component (duskward) of the electric field is largest. Because the long (spin plane) booms make the most accurate measurement of the quasi-static electric field, on the Van Allen Probes, E_y and E_z are most accurate, whereas on MMS E_y and E_x are most accurate. The well-measured E_z (VAP) and E_x (MMS) are both ~20% of E_y during the initial compression. The size of the magnetic field compressions, i.e., the difference between the observed field and the model magnetic field, is the same (~30 nT) at VAP-A and -B, and the perturbations in the *x* and *y* components were ~1 nT. At MMS, the values were larger, respectively, ~45 nT, and ~4 to ~6 nT. The electric field perturbation does not scale with the magnetic field compression.

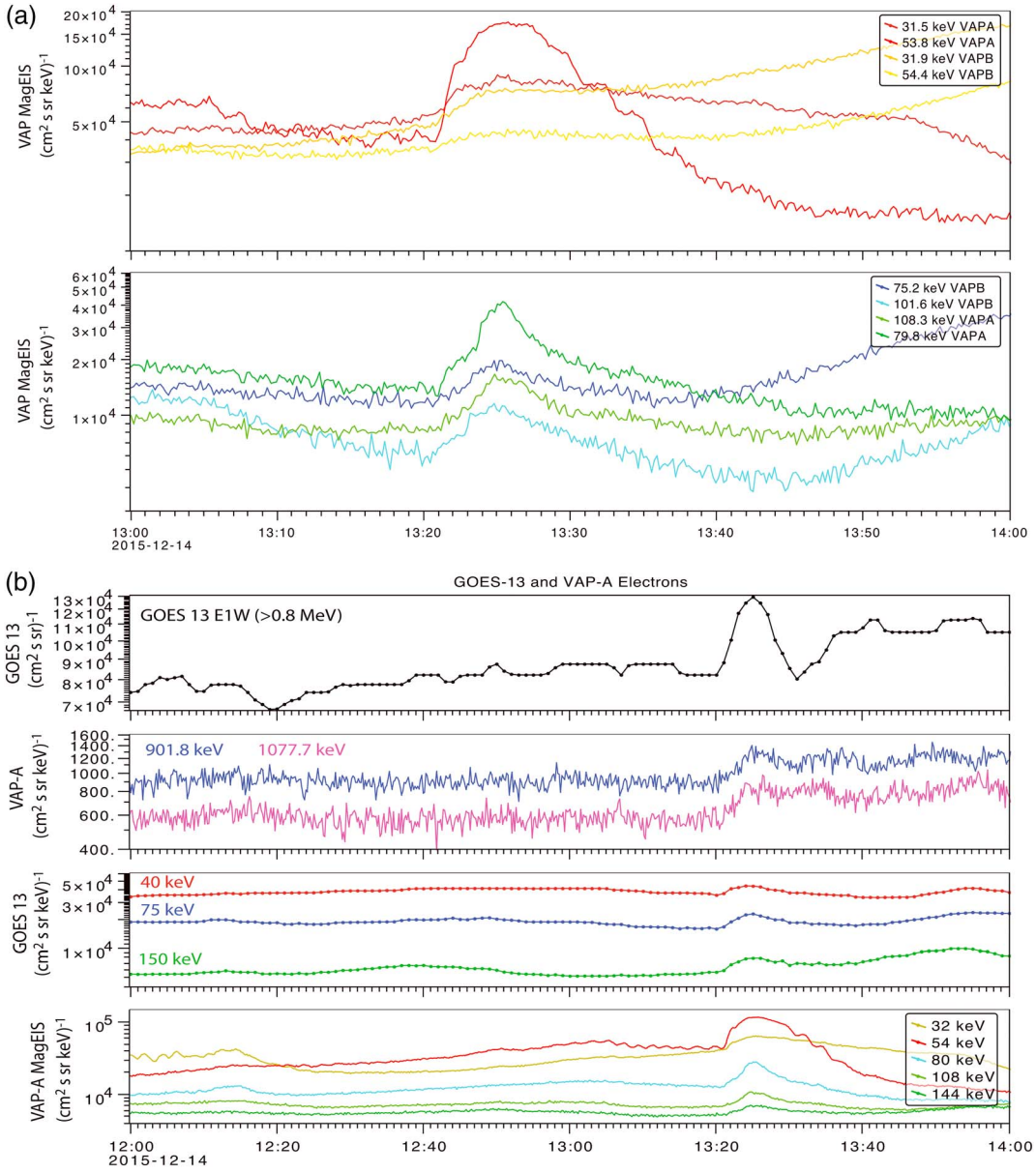

Figure 3. (a) Selected energy channels from MagEIS electrons at 90° PA, comparing VAP-A and B (top panel shows ~30 and ~50 keV; bottom shows ~70 and ~100 keV). (b) Comparison of VAP-A and GOES-13 electrons. (b, first panel) The >0.8 MeV fluxes from GOES-13, (b, second panel) the VAP-A 90° pitch angle fluxes at comparable energies (~0.9 MeV to ~1.6 MeV), (b, third panel) the GOES-13 fluxes at energies of ~40, 75, and 150 keV, and (b, fourth panel) the VAP-A 90° pitch fluxes at 32, 54, and 80 keV.

3. Discussion and Conclusions

The typically reported signature in the electric field in response to an interplanetary shock compression is a bipolar pulse, first dawnward and then duskward, usually with comparable amplitudes. This signature is interpreted to be due to a fast mode wave associated with the initial compression (tailward flow and Poynting flux), followed by the relaxation (and sunward flow). The initial signature is often followed by a train of ULF waves [*Wygant et al.*, 1994] and/or EMIC waves. In contrast, in this small shock, the initial response is a dawnward electric field with a double-peak structure, and there is no comparable size and duration duskward field. EMIC waves and ULF waves were observed.

A very similar signature in response to a small shock (~4 nPa) was observed on 9 January 2014 by VAP-B at ~13.5 MLT [*Halford et al.*, 2015]. This shock was also highly oblique. The initial field was primarily

dawnward (~6 mV/m) with a double pulse, followed by a smaller (~2 mV/m) duskward field. The initial magnetic field compression was ~5–10 nT, with an increase of ~30 nT over 5 min. The observed perturbations were consistent with initial fast mode propagation toward the nightside, followed by a rarefaction wave with return flow. VAP-A, which was at ~15 MLT, saw a single pulse structure. The initial magnetic field compression was simultaneous on both Van Allen Probes (separated by ~0.8 *Re*); however, the response in both the electric and magnetic field was of longer duration on VAP-A. The duskward electric field, E_y, was smaller at VAP-A (~ −2 mV/m) compared to ~ −6 mV/m at VAP-B.

The initial electric field response to both the 14 December 2015 and 9 January 2014 small shocks was consistent in amplitude and sign of electric field and magnetic field with a GEOS statistical study [*Schmidt and Pedersen*, 1988]. The perturbations were also consistent, when scaled by shock size, with simulations. Note that small shocks can also show a response similar to the typically reported bipolar electric field [*Zong et al*., 2009].

Both the 14 December 2015 and 9 January 2014 small shocks resulted in prompt enhancements in energetic electrons, although much less intense than those observed for moderate and large shocks. This is consistent with the statistical study of *Schiller et al*. [2016], who found that the size of the prompt enhancements was dependent on shock strength.

Simulations by *Kim et al*. [2009] examined the local time dependence of the electric field response to a moderate shock with an increase of ~10 nPa. They concluded that the bipolar pulse was not due to a compression followed by rarefaction. *Kim et al*. [2012] also reached conclusions at variance with usual interpretations. Utilizing magnetic field data from four widely spaced satellites on the dayside, they found that the propagation was slower than the fast mode speed.

For the event discussed herein, the compression moved the magnetopause inside 8 *Re*, so MMS moved into the magnetosheath and back into the magnetosphere. The speeds of the magnetopause crossings were subsonic, in agreement with previous statistical studies of magnetopause speeds [*Elphic*, 1988]. The initial compression of the magnetopause was roughly twice as fast as the relaxation.

Analysis of solar wind data from ARTEMIS (THEMIS-B and THEMIS-C), Wind, and ACE indicates that the shock was inclined and would likely have initially impacted the dawnside of the magnetosphere first, as was the case for the 7 October 2013 event studied by *Foster et al*. [2015]. Studies of the effect of shock angle on the response of the magnetosphere [*Takeuchi et al*., 2002; *Oliveira and Raeder*, 2015; *Samsonov et al*., 2015] indicate that shock angle can have a significant influence on the magnetospheric response.

Two large-scale MHD models have been run for this event at the CCMC (SWMF v20140611 and LFM LTR-2_1_15). Both show that the subsolar magnetopause is compressed to ~8.5 *Re*. Neither replicate the magnetopause crossing seen by MMS or the double-peaked dawnward electric field. The magnitudes of the initial dawnward fields are comparable for the two models and VAP-A; however, both models underestimate the electric field on MMS and on VAP-B. Possible explanations are that the models assume that the shock hits the Earth straight on (shock front is oriented with normal along the Earth-Sun line), whereas the observed shock was highly inclined, or that the spatial/temporal resolutions are not small enough to capture these structures, or that the modeled plasmasphere does not properly represent the effect of the real plasmasphere for this event. For example, *Kress et al*. [2007] found that the amplitude of the electric field response depended on the plasmasphere model. *Samsonov et al*. [2007] discussed the possible effect of wave reflection from the inner boundary (plasmapause or ionosphere).

The typical bipolar signature [*Wygant et al*., 1994; *Foster et al*., 2015] is also observed in MHD simulations of shock impacts [*Hudson et al*., 2015]. Simulation of the event described in *Foster et al*. [2015] by *Hudson et al*. [2015] showed that the pressure pulse of ~20 nPa resulted in bipolar pulse of ~8 mV/m comparable to the observed field. The initial dawnward pulse propagates in the fast mode azimuthally. The simulated pulse speed is 700 km/s comparable to the observed value of approximately 850 km/s [*Paral et al*., 2015]. VAP-B, farther from noon than VAP-A, observed a double dawnward pulse that was not replicated by the simulations.

These observations demonstrate that the response of the magnetosphere to interplanetary shocks can be highly variable. Even very weak shocks can cause enhancements in energetic electrons. To understand the

significance of IP shocks on radiation belt, dynamics and magnetic storms will require examination of a large number of events to assess the relative effect of various shock parameters and preexisting magnetospheric conditions.

Acknowledgments
The authors thank J.H. King and N. Papatashvilli at AdnetSystems and NASA/GSFC for access to the OMNI data through CDAWeb and the World Data Center. We also thank the EFW instrument teams at Space Sciences Lab of UCB and LASP of CU, the EMFISIS suite teams at University of Iowa and UNH, and the APL satellite team. The Van Allen Probes data sets are available from http://www.space.umn.edu/rbspefw-data/, http://emfisis.physics.uiowa.edu/data/ and https://rbsp-ect.lanl.gov/science/DataDirectories.php; GOES-13 data were obtained from https://satdat.ngdc.noaa.gov/sem/goes/, Wind and ACE data were obtained from http://cdaweb.gsfc.nasa.gov/, ARTEMIS data are available from http://themis.ssl.berkeley.edu/overview_data.shtml, and MMS data are available from https://lasp.colorado.edu/mms/sdc/public/. Work at the University of Minnesota was supported contract from APL, under NASA prime contact NAS5-01072. The work at Aerospace was supported in part by contract 792084 N/E99017JD from Southwest Research Institute (MMS/FEEPS), and JHU/APL contract 967399 (RBSP/MagEIS and ECT). MMS work at SWRI was supported by NASA contract NNG04EB99C.

References

Anderson, B. J., and D. C. Hamilton (1993), Electromagnetic ion cyclotron waves stimulated by modest magnetospheric compressions, *J. Geophys. Res.*, *98*(A7), 11,369–11,382, doi:10.1029/93JA00605.

Angelopoulos, V. (2008), The THEMIS Mission, *Space Sci. Rev.*, *141*, 5–34.

Baker, D. N., et al. (2012), The Relativistic Electron-Proton Telescope (REPT) Instrument on board the Radiation Belt Storm Probes (RBSP) Spacecraft: Characterization of Earth's radiation belt high-energy particle populations, *Space Sci. Rev.*, *179*, 337–381.

Blake, J. B., et al. (2013), Magnetic Electron Ion Spectrometer (MagEIS) instruments aboard the Radiation Belt Storm Probes (RBSP) spacecraft, *Space Sci. Rev.*, doi:10.1007/s11214-013-9991-8.

Burch, J. L., T. E. Moore, R. B. Torbert, and B. L. Giles (2015), Magnetospheric Multi-Scale overview and science objectives, *Space Sci. Rev.*, *199*, 5–21, doi:10.1007/s11214-015-0164-9.

Capman, N., et al. (2016), MMS, Van Allen Probes, and ground based magnetometer observations of a compression-induced EMIC wave event, SM13B-2207, Fall AGU.

Elphic, R. C. (1988), Multipoint observations of the magnetopause: Results from ISEE and AMPTE, *Space Res.*, *8*(9–10), (9)223–(9)238.

Foster, J. C., J. R. Wygant, M. K. Hudson, A. J. Boyd, D. N. Baker, P. J. Erickson, and H. E. Spence (2015), Shock-induced prompt relativistic electron acceleration in the inner magnetosphere, *J. Geophys. Res. Space Physics*, *120*, 1661–1674, doi:10.1002/2014JA020642.

Funsten, H. O., et al. (2013), Helium, Oxygen, Proton, and Electron (HOPE) mass spectrometer for the Radiation Belt Storm Probes mission, *Space Sci. Rev.*, *179*, 423–484, doi:10.1007/s11214-013-9968-7.

Halford, A. J., et al. (2015), BARREL observations of an ICME-shock impact with the magnetosphere and the resultant radiation belt electron loss, *J. Geophys. Res. Space Physics*, *120*, doi:10.1002/2014JA020873.

Hudson, M. K., J. Paral, B. T. Kress, M. Wiltberger, D. N. Baker, J. C. Foster, D. L. Turner, and J. R. Wygant (2015), Modeling CME-shock-driven storms in 2012–2013: MHD test particle simulations, *J. Geophys. Res. Space Physics*, *120*, 1168–1181, doi:10.1002/2014JA020833.

Kim, K.-H., et al. (2012), Magnetospheric responses to the passage of the interplanetary shock on 24 November 2008, *J. Geophys. Res.*, *117*, A10209, doi:10.1029/2012JA017871.

Kim, K.-H., K. S. Park, T. Ogino, D.-H. Lee, S.-K. Sung, and Y.-S. Kwak (2009), Global MHD simulation of the geomagnetic sudden commencement on 21 October 1999, *J. Geophys. Res.*, *114*, A08212, doi:10.1029/2009JA014109.

Kletzing, C. A., et al. (2013), The Electric and Magnetic Field Instrument Suite and Integrated Science (EMFISIS) on RBSP, *Space Sci. Rev.*, *179*, doi:10.1007/s11214-013-9993-6.

Kress, B. T., M. K. Hudson, M. D. Looper, J. Albert, J. G. Lyon, and C. C. Goodrich (2007), Global MHD test particle simulations of >10 MeV radiation belt electrons during storm sudden commencement, *J. Geophys. Res.*, *112*, A09215, doi:10.1029/2006JA012218.

Kurth, W. S., S. De Pascuale, J. B. Faden, C. A. Kletzing, G. B. Hospodarsky, S. Thaller, and J. R. Wygant (2015), Electron densities inferred from plasma wave spectra obtained by the Waves instrument on Van Allen Probes, *J. Geophys. Res. Space Physics*, *120*, 904–914, doi:10.1002/2014JA020857.

Lepping, R. P., et al. (1995), The wind magnetic field investigation, *Space Sci. Rev.*, *71*, 207–229, doi:10.1007/BF00751330.

Li, X., I. Roth, M. Temerin, J. R. Wygant, M. K. Hudson, and J. B. Blake (1993), Simulation of the prompt energization and transport of radiation belt particles during the March 24, 1991 SSC, *Geophys. Res. Lett.*, *20*, 2423–2426, doi:10.1029/93GL02701.

Lindqvist, P.-A., et al. (2015), The spin-plane double probe electric field instrument for MMS, *Space Sci. Rev.*, doi:10.1007/s11214-014-0116-9.

McFadden, J. P., C. W. Carlson, D. Larson, M. Ludlam, R. Abiad, B. Elliott, P. Turin, M. Marckwordt, and V. Angelopoulos (2008), The THEMIS ESA plasma instrument and in-flight calibration, *Space Sci. Rev.*, *141*, 277–302, doi:10.1007/s11214-008-9440-2.

Oliveira, D. M., and J. Raeder (2015), Impact angle control of interplanetary shock geoeffectiveness: A statistical study, *J. Geophys. Res. Space Physics*, *120*, 4313–4323, doi:10.1002/2015JA021147.

Paral, J., M. K. Hudson, B. T. Kress, M. J. Wiltberger, J. R. Wygant, and H. J. Singer (2015), Magnetohydrodynamic modeling of three Van Allen Probes storms in 2012 and 2013, *Ann. Geophys.*, *33*, 1037–1050, doi:10.5194/angeo-33-1037-2015. [Available at http://www.ann-geophys.net/33/1037/2015/.]

Russell, C. T., et al. (2014), The Magnetospheric Multi-Scale magnetometers, *Space Sci. Rev.*, *199*, 189–256, doi:10.1007/s11214-014-0057-3.

Samsonov, A. A., V. A. Sergeev, M. M. Kuznetsova, and D. G. Sibeck (2015), Asymmetric magnetospheric compressions and expansions in response to impact of inclined interplanetary shock, *Geophys. Res. Lett.*, *42*, 4716–4722, doi:10.1002/2015GL064294.

Samsonov, A. A., D. G. Sibeck, and J. Imber (2007), MHD simulation for the interaction of an interplanetary shock with the Earth's magnetosphere, *J. Geophys. Res.*, *112*, A12220, doi:10.1029/2007JA012627.

Schiller, Q., S. G. Kanekal, L. K. Jian, X. Li, A. Jones, D. N. Baker, A. Jaynes, and H. E. Spence (2016), Prompt injections of highly relativistic electrons induced by interplanetary shocks: A statistical study of Van Allen Probes observations, *Geophys. Res. Lett.*, *43*, 12,317–12,324, doi:10.1002/2016GL071628.

Samsonov, A. A., D. G. Sibeck, B. M. Walsh, and N. V. Zolotova (2014), Sudden impulse observations in the dayside magnetosphere by THEMIS, *J. Geophys. Res. Space Physics*, *119*, 9476–9496, doi:10.1002/2014JA020012.

Schmidt, R., and A. Pedersen (1988), Signatures of storm sudden commencements in the electric field measured at geostationary orbit (GEOS-2), *Phys. Scr.*, *37*, 491–495.

Singer, H., L. Matheson, R. Grubb, A. Newman, and D. Bouwer (1996), Monitoring space weather with the GOES magnetometers, Proc. SPIE 2812, GOES-8 and Beyond, 299 (October 18, 1996); doi:10.1117/12.254077.

Spence, H. E., et al. (2013), Science goals and overview of the Radiation Belt Storm Probes (RBSP) Energetic Particle, Composition, and Thermal Plasma (ECT) Suite on NASA's Van Allen Probe mission, *Space Sci. Rev.*, doi:10.1007/s11214-013-0007-5.

Stone, E. C., A. M. Frandsen, R. A. Mewaldt, E. R. Christian, D. Margolies, J. F. Ormes, and F. Snow (1998), The advanced composition explorer, *Space Sci. Rev.*, *86*(1/4), 1–22, doi:10.1023/A:1005082526237.

Takeuchi, T., C. T. Russell, and T. Araki (2002), Effect of the orientation of interplanetary shock on the geomagnetic sudden commencement, *J. Geophys. Res.*, *107*(A12), 1423, doi:10.1029/2002JA009597.

Torbert, R., et al. (2015), The FIELDS instrument suite on MMS: Scientific objectives, measurements, and data products, *Space Sci Rev.*, doi:10.1007/s11214-014-0109-8.

Wygant, J. R., et al. (2013), The Electric Field and Waves (EFW) instruments on the Radiation Belt Storm Probe mission, *Space Sci. Rev.*, doi:10.1007/s1124-013-0013-7.

Wygant, J., F. Mozer, M. Temerin, J. Blake, N. Maynard, H. Singer, and M. Smiddy (1994), Large amplitude electric and magnetic field signatures in the inner magnetosphere during injection of 115 MeV electron drift echoes, *Geophys. Res. Lett.*, *21*, 1739–1742, doi:10.1029/94GL00375.

Zong, Q.-G., X.-Z. Zhou, Y. F. Wang, X. Li, P. Song, D. N. Baker, T. A. Fritz, P. W. Daly, M. Dunlop, and A. Pedersen (2009), Energetic electron response to ULF waves induced by interplanetary shocks in the outer radiation belt, *J. Geophys. Res.*, *114*, A10204, doi:10.1029/2009JA014393.